

Published in final edited form as:

*Transplantation*. 2009 June 15; 87(11): 1659–1666. doi:10.1097/TP.0b013e3181a5cbc0.

## In vivo imaging of autologous islet grafts in the liver and under the kidney capsule in non-human primates

Zdravka Medarova<sup>1,\*</sup>, Prashanth Vallabhajosyula<sup>2,\*</sup>, Aseda Tena<sup>2</sup>, Natalia Evgenov<sup>1</sup>, Pamela Pantazopoulos<sup>1</sup>, Vaja Tchiphashvili<sup>3</sup>, Gordon Weir<sup>3</sup>, David Sachs<sup>2</sup>, and Anna Moore<sup>1,#</sup>

<sup>1</sup>Molecular Imaging Laboratory, MGH/MIT/HMS Athinoula A. Martinos Center for Biomedical Imaging, Department of Radiology, Massachusetts General Hospital/Harvard Medical School, Boston MA

<sup>2</sup>Transplantation Biology Research Center, Massachusetts General/Hospital/Harvard Medical School, Boston MA

<sup>3</sup>Section on Islet Transplantation and Cell Biology, Joslin Diabetes Center, Harvard Medical School, Boston MA

### Abstract

**Objective**—As islet transplantation begins to show promise clinically, there is a critical need for reliable, non-invasive techniques to monitor islet graft survival. Previous work in our laboratory has shown that human islets labeled with a superparamagnetic iron oxide contrast agent and transplanted into mice could be detected by magnetic resonance imaging (MRI). The potential translation of these findings to the clinical situation requires validation of our methodology in a non-human primate model, which we have now carried out in baboons (*Papio hamadryas*) and reported here.

**Research Design and Methods:** For islet labeling, we adapted the FDA-approved superparamagnetic iron oxide contrast agent, Feridex, which is used clinically for liver imaging. After partial pancreatectomy, Feridex-labeled islets were prepared and autotransplanted underneath the renal capsule and into the liver. Longitudinal in vivo MRI at days 1, 3, 8, 16, 23, and 30 after transplantation was performed in order to track the islet grafts.

**Results**—The renal subcapsular islet graft was easily detectable on T2\*-weighted MRI images as a pocket of signal loss disrupting the contour of the kidney at the transplantation site. Islets transplanted in the liver appeared as distinct signal voids dispersed throughout the liver parenchyma. A semi-automated computational analysis of our MR imaging data established the feasibility of monitoring both the renal and intrahepatic grafts during the studied post-transplantation period.

**Conclusion**—This study establishes a method for the noninvasive, longitudinal detection of pancreatic islets transplanted into non-human primates using a low field clinical MRI system.

# Correspondence should be addressed to: Anna Moore, Ph.D., MGH/MIT/HMS Athinoula A. Martinos Center for Biomedical Imaging, Department of Radiology, Massachusetts General Hospital/Harvard Medical School, Rm. 2301, Bldg.149, 13th St., Charlestown, Massachusetts 02129, Tel:(617)724-0540, Fax:(617)726-7422, amoores@helix.mgh.harvard.edu.

\*These authors contributed equally

Zdravka Medarova performed the MRI experiments and participated in experimental design and the writing of the manuscript; Prashanth Vallabhajosyula performed animal surgery and participated in experimental design and the writing of the manuscript; Aseda Tena was responsible for animal care and participated in animal surgery; Natalia Evgenov performed islet labeling and in vitro experiments; Pamela Pantazopoulos performed the ex vivo histology studies; Vaja Tchiphashvili was responsible for islet isolation; Gordon Weir, David Sachs, and Anna Moore participated in experimental design and the writing of the manuscript; Anna Moore conceived the idea for the study.

## Keywords

islet; islet labeling; feridex; islet transplant; MRI; non-human primate

---

## Introduction

Islet transplantation has emerged as a promising treatment modality in a select population of patients with type 1 diabetes. Although the introduction of the immunosuppressive regimen known as the Edmonton protocol (1) showed promising results, further follow-up has revealed that 75% of the patients were insulin independent at one year post-transplantation (2). A more recent international trial using the Edmonton protocol showed that only 44% of patients receiving islet transplantation remained insulin independent at one year post-transplant (3). Therefore, although relatively successful, this protocol still suffers from significant graft loss and/or islet injury that occur during the peri- and post-transplant period and that adversely affects the long-term outcome in transplant recipients.

One of the problems in this field is the inability to track rejection/ islet loss non-invasively in a timely manner. Our group has previously developed a method to detect transplanted human islets labeled with superparamagnetic iron oxide nanoparticles non-invasively in mice, using magnetic resonance imaging (MRI) (4,5). We showed that islet rejection could be reliably monitored by in vivo MR imaging (6). These studies attempting to visualize individual transplanted islets directly used a spatial resolution comparable to the dimensions of a typical islet. For adequate contrast, they relied on the so-called “blooming effect” associated with the detection of superparamagnetic iron oxide contrast agents using T2/T2\*-weighted MRI sequences. This effect is well described and results in a susceptibility footprint on MR images, which is larger than the actual entity containing the contrast agent (7). In our reports, labeled islets (150-200  $\mu\text{m}$  in diameter) were easily detected within a  $125 \times 125 \times 500 \mu\text{m}$  imaging voxel (6), as a consequence of the “blooming effect”. However, the translation of this new technology to the clinic where the use of clinical, low-field MRI is necessary poses considerable challenges, in terms of spatial resolution, magnetic susceptibility and signal-to-noise. Combined, these factors result in a reduced probability of islet detection, as the magnitude of the “blooming effect” is dependent on susceptibility/field-strength, as well as local iron concentration (7). In addition, automated image analysis relevant to the potential future clinical applicability of the technology has to be developed.

With these considerations in mind, we have developed a comprehensive new method for visualization of transplanted islets in a large animal model. As a labeling contrast agent we utilized the Food and Drug Administration (FDA) approved contrast agent, Feridex, which is routinely used in the clinical setting for liver imaging. In a pre-clinical non-human primate (baboon: *Papio hamadryas*) model of autologous islet transplantation, we show that islets labeled with Feridex can be detected in vivo by MRI. Furthermore, we describe the development of a semi-automated image analysis algorithm for the quantitative evaluation of change in transplanted islet mass over time. Finally, we demonstrate that the labeling technique is safe to the animal, and does not adversely affect the long-term function or survival of the animal and the transplanted islets. To our knowledge, this is the first report of successful in vivo MR imaging of transplanted islets in a pre-clinical, non-human primate model.

## Materials and Methods

### Baboon care and operative procedures

**Baboon care**—The baboons ( $n = 2$ ) were housed in an animal facility at the Massachusetts General Hospital (MGH), Boston. They were observed at least twice daily throughout the

follow-up period. After islet transplantation, the animals were monitored for signs of systemic problems. Periodically, the animals were sedated to obtain blood chemistries including fasting blood glucose (FBG), electrolytes, renal profile, liver profile, and complete blood count. All animal experiments were performed in compliance with institutional guidelines and were approved by the subcommittee on research animal care (SRAC) at the MGH.

**Islet harvest and autologous islet transplantation**—A 60-70% partial pancreatectomy was performed. The obtained tissue was used for islet isolation, labeling, and autologous transplantation underneath the kidney capsule (islet-kidney graft) and in the liver. In the first animal (B155), 25% of isolated islets (total = 160,000) were transplanted in the liver and 75% underneath the kidney capsule. In the second animal (B173), 75% of isolated islets (total = 160,000) were transplanted in the liver and 25% underneath the kidney capsule. Details of the partial pancreatectomy and islet transplantation procedures are described in Supplemental Materials and Methods.

**Completion pancreatectomy**—Completion pancreatectomy was performed according to established protocol. Details of the surgical procedure are described in Supplemental Materials and Methods.

### Labeling baboon islets with the contrast agent, Feridex

Baboon islets were isolated at Joslin Diabetes Center, Boston. (8) Islets were cultured overnight in Miami Medium #1 culture media (Cellgro; Mediatech, Herndon, VA) supplemented with ciprofloxacin (20 mg/L; Fisher Scientific, Pittsburgh, PA) and L-glutathione (10 mg/L; Sigma, St. Louis, MO). For labeling experiments, nanoparticulate superparamagnetic iron oxide, Feridex (ferumoxide; Advanced Magnetics, Cambridge, MA), was added to the culture media at an iron concentration of 400 µg/ml. After overnight culture, the labeled islets were washed 3 times in Hanks Balanced Salt Solution (HBSS) and used either for in vitro experiments or islet transplantation. A small fraction of the isolated islets were unlabeled to serve as controls for the in vitro assays.

### In vitro islet analysis

**Islet count, islet purity and viability**—*Islet count, islet purity and viability* were assessed using standard procedures and described in detail in Supplemental Materials and Methods

**Insulin secretion**—Labeled and unlabeled islets were incubated in static conditions at low and high glucose concentrations. The procedure is described in detail in Supplemental Materials and Methods.

**Iron retention assay**—Aliquots of 100 islets (in triplicates) were incubated overnight with 200 µg/ml of Feridex, washed in PBS, resuspended in culture media, and assayed for iron content at various time-points (up to 24 hours) to measure for any iron loss. Iron uptake was measured using total iron reagent set (Pointe Scientific, Canton, MI).

**Apoptosis assay**—A fluorometric caspase-3 assay (Sigma) was utilized to measure apoptosis in labeled and unlabeled islets. Baboon islets were labeled with 400 µg/ml Feridex for 0, 1, 2, 4, 6, and 24 hours, lysed, and assayed per manufacturer's protocol. Islets incubated with 1 µg/ml of staurosporine served as positive control.

## In vivo MR imaging and image analysis

During imaging the animal was maintained on propofol sedation. Details of animal handling before, during, and immediately after imaging are described in Supplemental Materials and Methods.

**MR imaging**—In vivo MR imaging was performed before and at multiple time points after transplantation using a 1.5T Siemens magnet (6 channel body matrix coil and a spine-array coil). The details of the imaging parameters are presented in Supplemental Materials and Methods.

## Image analysis

Image analysis was performed using the FreeSurfer 3.0.4 interactive graphical user interface (GUI), Scuba (9,10). For details, see Supplemental Materials.

## Results

### Labeling of baboon islets with Feridex

To test the success of the labeling process with Feridex and its effect on baboon islet function, in vitro analyses were performed. The amount of iron associated with the islets and measured up to 24 hours post-labeling, showed that the iron content of baboon islets remained constant after incubation in culture for 24 hours ( $p > 0.05$ , Fig. 1A). The labeling process did not affect islet viability as assessed by staining with difluoroacetate and propidium iodide (data not shown). Furthermore, an apoptosis assay confirmed that labeling islets with Feridex up to 24 hours did not increase the apoptotic rate in labeled compared to unlabeled islets ( $p > 0.05$ , Fig. 1B). To ensure that Feridex labeling does not adversely affect islet function, glucose-stimulated insulin release was measured on labeled and unlabeled baboon islets. The stimulation index was unchanged in labeled versus unlabeled islets ( $p > 0.05$ , Fig. 1C). These experiments suggested that labeling baboon islets with Feridex does not adversely affect islet viability or islet function similar to our previous findings with human islets (4,6).

### In vivo imaging of labeled islets auto-transplanted underneath the kidney capsule and into the liver

**Islet transplantation under the kidney capsule**—On T2\*-weighted MR images, islets transplanted underneath the renal capsule appeared as a pocket of signal loss disrupting the contour of the kidney (Fig. 2A). This was in stark contrast to the pre-transplant scan, where the left kidney had a smooth homogenous contour on MRI. The contralateral kidney, without any islet injection, showed no change before and after transplantation. The site of the signal void correlated with the anatomic site of islet transplantation in the renal capsule. The renal subcapsular graft was closely monitored through serial MRI. The T2\* signal void was consistently detected on MRI, and was absent in the contralateral kidney. Signal coming from the graft was detectable throughout the follow-up period.

**Intrahepatic islet transplantation**—Islets transplanted intrahepatically appeared as distinct areas of signal loss, seen as signal voids dispersed throughout the liver (Fig. 2B). By contrast, on pre-transplant T2\*-weighted images, the liver parenchyma was characterized by considerable homogeneity (Fig. 2B). After transplantation, the highest concentration of islets was seen in the right posterior hepatic lobes. At the time of transplantation the animal was placed in a supine position. As the infused islets lodge into the portal branches, due to gravity, likely the heavier islets drained downwards towards the posterior lobes of the liver. We were also able to track the intrahepatic islet graft over time by serial MRI. On these images islets continued to appear as signal voids throughout the liver. With these results we established that

labeled islets, when transplanted into the liver or kidney of a non-human primate, could be clearly detected in vivo and the signal can be tracked over time using MRI.

**Computational MR image analysis**—In the mouse transplantation model, we were able to quantify relative transplanted islet mass by manually scoring the number of hypointense voxels representing islet graft on MR images, and then tracking this value over time (6). Clearly, this method is impractical in a large animal model or in a potential clinical situation. Therefore, we developed a semi-automated image segmentation algorithm for the reliable identification of image voxels occupied by the graft and quantitative analysis of their relative abundance over time. Using an automated segmentation method, K-means (based on MatLab), the kidney and the liver were each classified into two labels based on their T2\* values: the islet graft label and the renal parenchyma (Fig. 3A), or the islet graft label and the liver parenchyma (Fig. 3B). Our initial analysis indicated that the T2\* values associated with the two labels were sufficiently distinct to allow precise differentiation between the two in both the kidney and the liver transplantation models ( $p < 0.05$ ). The final outcome was a first order estimate of the transplanted islet mass. This value could then be plotted over time to track relative transplanted islet mass, as measured by MRI.

Our analysis revealed a relative stability in islet mass transplanted underneath the renal capsule during the initial (30 days) posttransplant period (Fig. 4A), which was consistent with our previous report in the murine model (4). In the intrahepatic model, we observed a noticeable 25% drop in transplanted islet mass between days 3 and 8 after transplantation, consistent with our previous results in the immunocompromised murine model (6). This was followed by stabilization of the graft over the observation period (Fig. 4B).

### Long-term safety of transplanting Feridex-labeled islets

After autologous transplantation of labeled islets the baboons were monitored for long-term in order to evaluate the in vivo safety profile of transplanted Feridex-labeled islets. Periodic complete blood counts were obtained throughout the follow-up. The animals showed no signs of infection, maintaining normal white blood cell counts without neutrophilia (Fig. 5A). The animals showed no signs of anemia or thrombocytopenia (Fig. 5A) or any symptoms of systemic inflammation such as elevated C reactive protein levels (data not shown). They also maintained normal weight gain during the follow-up suggesting that they remained in an anabolic state during the post-transplantation period (data not shown). They had normal total protein levels and normal lipid metabolism during the follow-up, while changes in triglycerides and cholesterol levels were transient and associated with the surgical transplantation procedure, with normalization thereafter (Fig. 5B).

Since the labeled islets were transplanted into the liver and underneath the renal capsule, we also followed liver and renal function tests to ensure that there was no organ specific damage due to the labeled islets. Besides a transient increase in the levels of aspartate aminotransferase (AST), alanine aminotransferase (ALT) and bilirubin after the partial pancreatectomy, the liver function tests indicated no disruption in hepatic physiology (Fig. 5C). Blood urea nitrogen (BUN) and creatinine values remained within normal range during the follow-up period suggesting normal renal function (Fig. 5D).

### Feridex-labeled islets engraft post-transplantation and show long-term function

The animals maintained normal glucose homeostasis at baseline and normal glucose tolerance during the long-term follow-up (Fig. 6). Pre-transplant and post-transplant fasting blood glucose values were normal (Fig. 6A) and the response to glucose challenge on intravenous glucose tolerance tests was unremarkable and unchanged (Fig. 6B).

Given that the baboons had 40% of their pancreas remaining after partial pancreatectomy, there was no way to discern for any contribution to glucose regulation made by the labeled transplanted islets as opposed to the remnant pancreatic stump. To assess if Feridex-labeled islets can maintain glucose homeostasis long-term, we performed completion pancreatectomy. The animals maintained normal fasting blood glucose values during the period following completion pancreatectomy.

One of the baboons was followed for >60 days after this procedure, and it consistently maintained normoglycemia, with fasting blood glucose <80 mg/dl, indicating that Feridex-labeled islets maintained their functionality (Fig. 6A). Intravenous glucose tolerance tests were also performed. There was no difference between pre- and post-completion pancreatectomy time points, despite the significant reduction in islet mass effected by the removal of the remaining endogenous pancreas (Fig. 6B). This result suggests that Feridex-labeled islets can successfully maintain long-term glucose homeostasis, with normal fasting glycemic control and an appropriate level of glucose tolerance upon challenge.

## Discussion

One of the major obstacles in islet transplantation is the inability to track the islet mass in an efficient, non-invasive manner. At present, our understanding of the performance of an islet graft is dependent on monitoring blood glucose values. Although increases in fasting blood glucose may be a good marker of islet graft dysfunction, unfortunately, interventions to reverse the ensuing hyperglycemia are often too late and thus unsuccessful. Any methods to reliably and non-invasively monitor the transplanted islet mass may greatly enhance our ability to intervene in a timely fashion. Numerous investigations towards that goal have been performed in the last few years (11-19). Bioluminescence and nuclear imaging have the advantages of being quantitative and sensitive to local contrast agent concentration. However, bioluminescence imaging is not clinically applicable (13,16,19) whereas nuclear imaging either requires genetic modification of the islets (14,15) or the application of radioactively-labeled contrast agents, whose retention time by the islets is likely too short for the long-term monitoring of graft fate (11,12). The latter issue is also a concern when using low-molecular weight gadolinium-based contrast agents for islet visualization by MRI (18).

Superparamagnetic iron oxides, which are the subject of the current investigation, have the advantages of being clinically applicable (20,21) and having a long retention time within the islets, permitting long-term studies. Superparamagnetic iron oxide agents can also be chemically modified with targeting moieties to impart to them cell specificity, i.e. to beta-cells within the islet, or to concurrently deliver molecular therapeutic capabilities for the enhancement of engraftment (22). The major disadvantage of superparamagnetic iron oxides as a contrast agent is the fact that they generate non-unique negative contrast, which is generally more difficult to identify against endogenous tissue background. Also, despite the fact that "target-able" iron oxides can be developed, the clinically relevant utilization of these agents is exclusively based on their non-targeted version. Therefore, currently labeling with iron oxides does not provide information about beta-cell functionality.

Following the first reports describing the feasibility of detecting pancreatic islets labeled with superparamagnetic iron oxides (23), our laboratory has investigated the utility of the method in a variety of pre-clinical contexts, using the mouse model (4-6,24). More recently, labeled islets transplanted underneath the rat kidney capsule were successfully visualized using a low field-strength, 1.5 Tesla (1.5T) MRI system (7). In addition, detection of human islets encapsulated in immunoprotective magnetocapsules containing ferumoxides has been reported (17). The contrast agent within the capsule permitted the tracking of the initial islet-containing magnetocapsule infusion and its engraftment into the liver. Importantly, these studies were done in a large animal model (swine). However, this approach does not permit for direct islet

visualization, since the contrast agent remains trapped inside the magnetocapsule and will be detected even in the case of islet death. Additionally, while encapsulation protects the islets from a recurring auto- or allo-/immune attack, it may interfere with islet revascularization after transplantation, which is a crucial element of successful engraftment and long-term function. The first attempt to image transplanted islets labeled with superparamagnetic iron oxide nanoparticles in humans, however, failed to demonstrate the expected correlation between the number of iron-loaded islets infused in the liver and the number of hypointense spots on MR images (25). Without the availability of quantitative analysis of the imaging data and with the lack of a clear understanding of the processes behind islet labeling, these studies in humans provided only a preliminary indication that islet visualization after intrahepatic transplantation is possible.

Having said that, we need to emphasize that in this study we monitored changes in transplanted islet mass over time but not absolute transplanted islet mass. To measure absolute islet mass it would be necessary to construct accurate calibration plots in which transplanted islet mass is correlated to MR signal immediately after transplantation. We have conducted similar calibration studies in small animals and have established a close relationship between the number of transplanted islets and the number of signal voids on MR images. We have also demonstrated that MR imaging is sensitive to a change of as little as 20% in absolute transplanted islet mass (6).

In addition to the MRI studies described above, nuclear imaging has shown promise as a pre-clinical (12) and clinical method for detecting transplanted islets (11). According to these reports, almost 50% of the islets are damaged and released the fluorodeoxyglucose (FDG) label within minutes after intraportal infusion. This approach, however, is only useful for the short-term monitoring of transplanted islet fate, since the persistence of the label in the islet cells is unknown. In the context of the present study, these results are not inconsistent with our findings since they focus on the loss of islet mass immediately after intraportal infusion. Our studies monitored the long-term dynamics of islet mass (days not minutes). Our findings of a general stability of the islet graft underneath the renal capsule and the loss of about 25% of intrahepatic islet mass in the first week after transplantation are consistent with earlier reports using small animal models and a variety of imaging modalities (4,6,13,16).

Although the techniques employed for the *in vivo* MR imaging of islets in mice may be complex, the translation of these methods to a large animal or human is an even more formidable task requiring the development of a novel imaging methodology, distinct from that applied in a small animal model and using high field strength MRI systems. The need to utilize a larger field of view when imaging a large animal is associated with a proportional reduction in spatial resolution for the same investment in time (26-28). In small animal imaging systems, a spatial resolution of  $125 \times 125 \times 500 \mu\text{m}^3$  can easily be achieved. By contrast, in clinical MRI systems, typical in-plane resolutions for abdominal imaging approach  $1 \times 1 \times 1\text{mm}^3$  (29). At this relatively low resolution, the possibility of achieving adequate balance between the increased volume of a voxel containing a labeled islet and the magnitude of MRI contrast associated with this islet becomes a new challenge. For example, with the increase in voxel volume, the possibility of volume-averaging signal abnormalities known as partial volume effects becomes more likely (26). In addition, the application of clinical-grade low-field strength MRI systems is accompanied by a reduced susceptibility/signal-to-noise ratio (30). As a general principle, there is a reduction in sensitivity, signal-to-noise, contrast, and resolution with the decrease in field strength (27,28,30,31).

In addition to resolving technical challenges stemming from the use of low-field systems, we needed to address biological questions taking into consideration the consequences of islet labeling with contrast agent. In the context of bridging our work in mouse studies to human

islet transplantation, we addressed these questions in a pre-clinical, large animal, non-human primate model of autologous islet transplantation: (1) Can non-human primate islets be safely labeled in vitro with the FDA approved contrast agent Feridex? If so, does that alter islet function and survival in vitro? (2) Does labeling islets with Feridex enable the in vivo detection and tracking of the transplanted islet mass through magnetic resonance imaging? (3) Do the transplanted labeled islets function in vivo and regulate glucose homeostasis long-term? (4) Is the transplantation of Feridex-labeled islets safe to the recipient animal long-term? In addressing these questions, we established the feasibility of using clinical-grade MR imaging systems to non-invasively detect islets labeled with Feridex in a large-animal model. We developed and validated this methodology, while at the same time demonstrating the long-term safety of the applied protocols. In addition, we created a new computational tool for quantitative analysis of change in transplanted islet mass over time in islet transplantation models in both the liver and the kidney.

We believe that the significance of our studies is two-fold: First, we have demonstrated the feasibility of directly visualizing small structures (pancreatic islets; 150-200  $\mu\text{m}$  in diameter) in large animals, using low field-strength clinical MRI systems. Second, with the use of a clinically relevant contrast agent, imaging parameters and instrumentation, we have established a comprehensive imaging paradigm for evaluation of islet graft survival and function, which has a direct and immediate applicability in a clinical setting.

In conclusion, this study describes the in vivo detection of transplanted Feridex-labeled pancreatic islets using clinical field strength MRI in a large animal model. These experiments represent an essential intermediate step before translating MR imaging of islet transplantation from experimental to clinical applications.

## Supplementary Material

Refer to Web version on PubMed Central for supplementary material.

## Acknowledgments

The authors would like to acknowledge technical support from Specialized Assay Core supported by 5P30 DK 36836 from NIH. We would like to thank Gheorghe Postelnicu, Ph.D. and Bruce Fischl Ph.D. for their exceptional contribution in the development of semi-automated image analysis. This study was supported in part by NIH 1RO1DK078615 to A.M.

## References

1. Shapiro AM, Lakey JR, Ryan EA, et al. Islet transplantation in seven patients with type 1 diabetes mellitus using a glucocorticoid-free immunosuppressive regimen. *N Engl J Med* 2000;343(4):230. [PubMed: 10911004]
2. Ryan EA, Lakey JR, Rajotte RV, et al. Clinical outcomes and insulin secretion after islet transplantation with the Edmonton protocol. *Diabetes* 2001;50(4):710. [PubMed: 11289033]
3. Shapiro AM, Ricordi C, Hering BJ, et al. International trial of the Edmonton protocol for islet transplantation. *N Engl J Med* 2006;355(13):1318. [PubMed: 17005949]
4. Evgenov NV, Medarova Z, Dai G, Bonner-Weir S, Moore A. In vivo imaging of islet transplantation. *Nat Med* 2006;12(1):144. [PubMed: 16380717]
5. Medarova Z, Evgenov NV, Dai G, Bonner-Weir S, Moore A. In vivo multimodal imaging of transplanted pancreatic islets. *Nat Protoc* 2006;1(1):429. [PubMed: 17406265]
6. Evgenov NV, Medarova Z, Pratt J, et al. In vivo imaging of immune rejection in transplanted pancreatic islets. *Diabetes* 2006;55(9):2419. [PubMed: 16936189]
7. Tai JH, Foster P, Rosales A, et al. Imaging islets labeled with magnetic nanoparticles at 1.5 Tesla. *Diabetes* 2006;55(11):2931. [PubMed: 17065328]



8. Koulmanda M, Smith RN, Qipo A, Weir G, Auchincloss H, Strom TB. Prolonged survival of allogeneic islets in cynomolgus monkeys after short-term anti-CD154-based therapy: nonimmunologic graft failure? *Am J Transplant* 2006;6(4):687. [PubMed: 16539625]
9. Fischl B, Sereno MI, Dale AM. Cortical surface-based analysis. II: Inflation, flattening, and a surface-based coordinate system. *Neuroimage* 1999;9(2):195. [PubMed: 9931269]
10. Dale AM, Fischl B, Sereno MI. Cortical surface-based analysis. I. Segmentation and surface reconstruction. *Neuroimage* 1999;9(2):179. [PubMed: 9931268]
11. Eich T, Eriksson O, Lundgren T. Visualization of early engraftment in clinical islet transplantation by positron-emission tomography. *N Engl J Med* 2007;356:2754. [PubMed: 17596618]
12. Eich T, Eriksson O, Sundin A, et al. Positron emission tomography: a real-time tool to quantify early islet engraftment in a preclinical large animal model. *Transplantation* 2007;84(7):893. [PubMed: 17984843]
13. Fowler M, Virostko J, Chen Z, et al. Assessment of pancreatic islet mass after islet transplantation using in vivo bioluminescence imaging. *Transplantation* 2005;79(7):768. [PubMed: 15818318]
14. Lu Y, Dang H, Middleton B, et al. Long-term monitoring of transplanted islets using positron emission tomography. *Mol Ther* 2006;14(6):851. [PubMed: 16982215]
15. Lu, Y.; Dang, H.; Middleton, B., et al. *Imaging the Pancreatic Beta Cell*. Bethesda, MD: 2003. Repetitive microPET imaging of implanted human islets in mice.
16. Lu Y, Dang H, Middleton B, et al. Bioluminescent monitoring of islet graft survival after transplantation. *Mol Ther* 2004;9:428. [PubMed: 15006610]
17. Barnett BP, Arepally A, Karmarkar PV, et al. Magnetic resonance-guided, real-time targeted delivery and imaging of magnetocapsules immunoprotecting pancreatic islet cells. *Nat Med*. 2007
18. Biancone L, Crich SG, Cantaluppi V, et al. Magnetic resonance imaging of gadolinium-labeled pancreatic islets for experimental transplantation. *NMR Biomed* 2007;20(1):40. [PubMed: 16986104]
19. Chen X, Zhang X, Larson CS, Baker MS, Kaufman DB. In vivo bioluminescence imaging of transplanted islets and early detection of graft rejection. *Transplantation* 2006;81(10):1421. [PubMed: 16732180]
20. de Vries IJ, Lesterhuis WJ, Barentsz JO, et al. Magnetic resonance tracking of dendritic cells in melanoma patients for monitoring of cellular therapy. *Nat Biotechnol* 2005;23(11):1407. [PubMed: 16258544]
21. Zhu J, Zhou L, XingWu F. Tracking neural stem cells in patients with brain trauma. *N Engl J Med* 2006;355(22):2376. [PubMed: 17135597]
22. Medarova Z, Kumar M, Ng SW, et al. Multifunctional magnetic nanocarriers for image-tagged SiRNA delivery to intact pancreatic islets. *Transplantation* 2008;86(9):1170. [PubMed: 19005396]
23. Jirak D, Kriz J, Herynek V, et al. MRI of transplanted pancreatic islets. *Magn Reson Med* 2004;52(6):1228. [PubMed: 15562474]
24. Evgenov NV, Pratt J, Pantazopoulos P, Moore A. Effects of glucose toxicity and islet purity on in vivo magnetic resonance imaging of transplanted pancreatic islets. *Transplantation* 2008;85(8):1091. [PubMed: 18431227]
25. Toso C, Vallee JP, Morel P, et al. Clinical magnetic resonance imaging of pancreatic islet grafts after iron nanoparticle labeling. *Am J Transplant* 2008;8(3):701. [PubMed: 18294167]
26. Hendrick, R. *Image contrast and noise*. Vol. 3d. St. Louis: Mosby; 1999.
27. Cunningham PM, Law M, Schweitzer ME. High-field MRI. *Orthop Clin North Am* 2006;37(3):321. [PubMed: 16846764]
28. Hu X, Norris DG. Advances in high-field magnetic resonance imaging. *Annu Rev Biomed Eng* 2004;6:157. [PubMed: 15255766]
29. Tanenbaum LN. Clinical 3T MR imaging: mastering the challenges. *Magn Reson Imaging Clin N Am* 2006;14(1):1. [PubMed: 16530631]
30. Merkle EM, Dale BM. Abdominal MRI at 3.0 T: the basics revisited. *AJR Am J Roentgenol* 2006;186(6):1524. [PubMed: 16714640]
31. Magee T, Shapiro M, Williams D. Comparison of high-field-strength versus low-field-strength MRI of the shoulder. *AJR Am J Roentgenol* 2003;181(5):1211. [PubMed: 14573405]

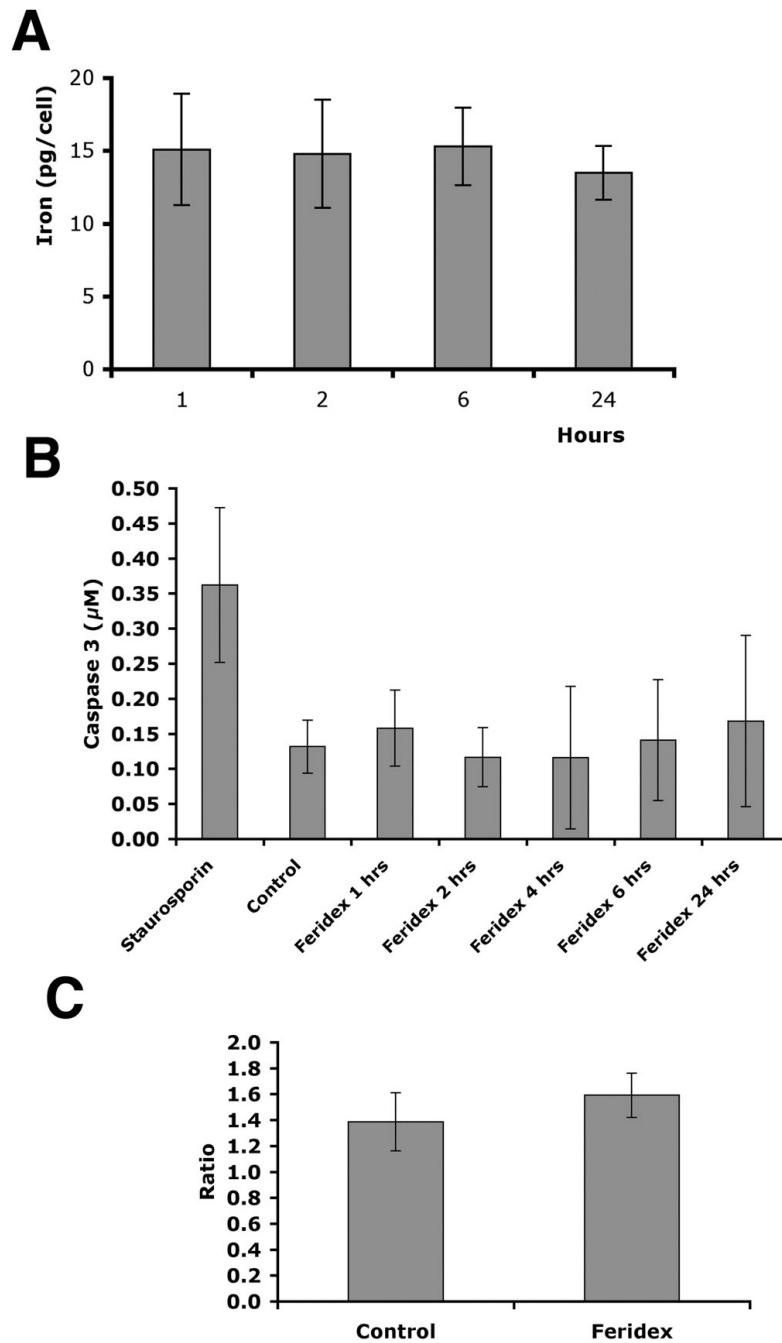


**Figure 1.**

In vitro labeling of baboon islets with Feridex. A: Baboon islets labeled with Feridex maintained the iron label over a period of 24 hours ( $n = 3$ ,  $p > 0.05$ ). B: Labeling of baboon islets with Feridex over a period of 24 hours did not lead to elevated apoptosis of islets compared to control, as shown by caspase-3 assay ( $n = 3$ ,  $p > 0.05$ ). Pancreatic islets treated with staurosporine ( $1\mu\text{g/ml}$ ) were used as a positive control. C: Glucose-stimulated insulin release was not significantly different between labeled and unlabeled islets ( $n = 3$ ,  $p > 0.05$ ).

pre-transplant

post-transplant

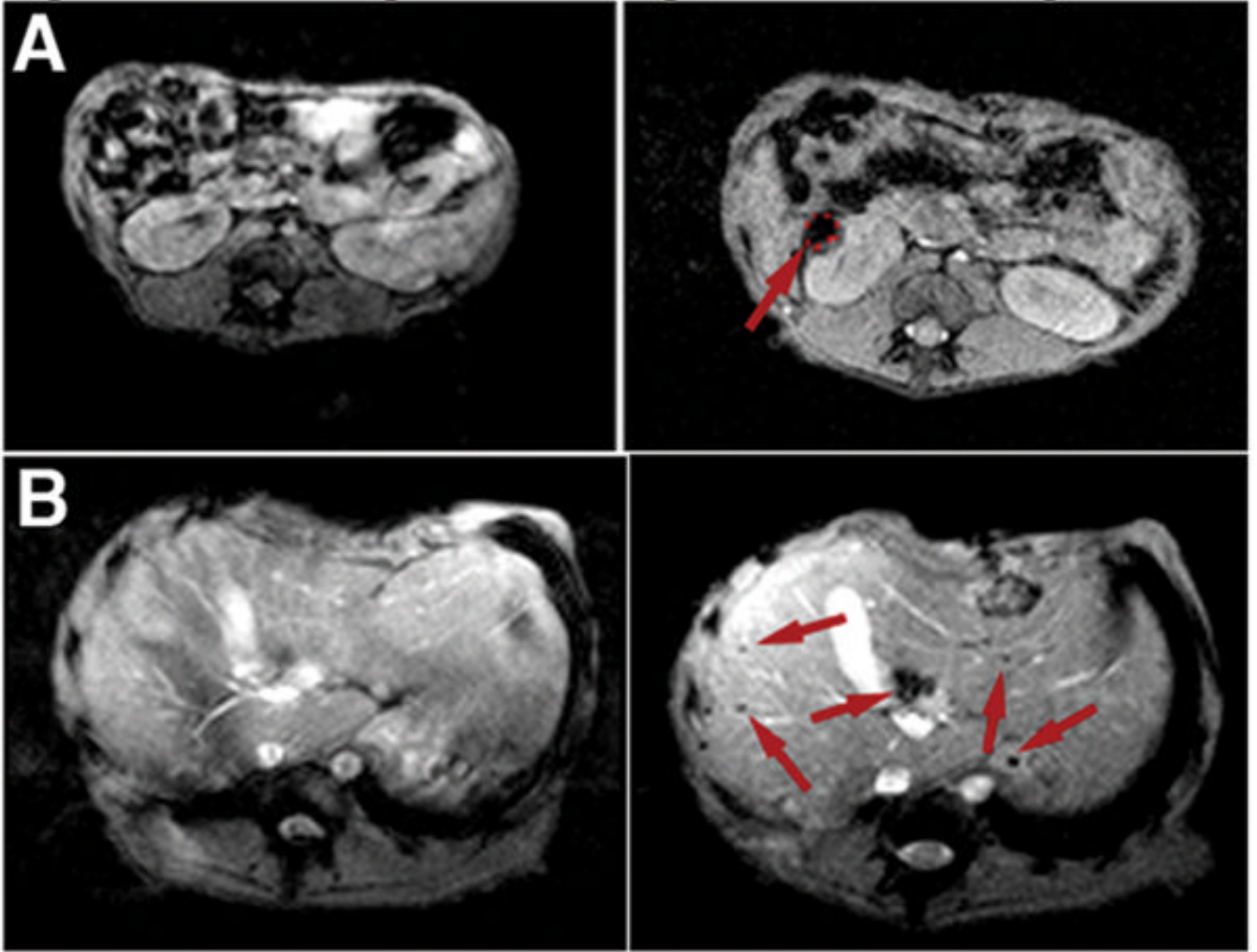


**Figure 2.** In vivo MR imaging of pancreatic islets autologously transplanted under the kidney capsule (A) or into the liver (B) of animal B173. The kidney graft (red outline and arrow) could be seen as a pocket of signal loss underneath the kidney capsule after but not before transplantation (A). In the liver, distinct foci of signal loss (arrows), representing labeled islets, could be identified after but not before transplantation, reflecting the presence and distribution of the graft (B).

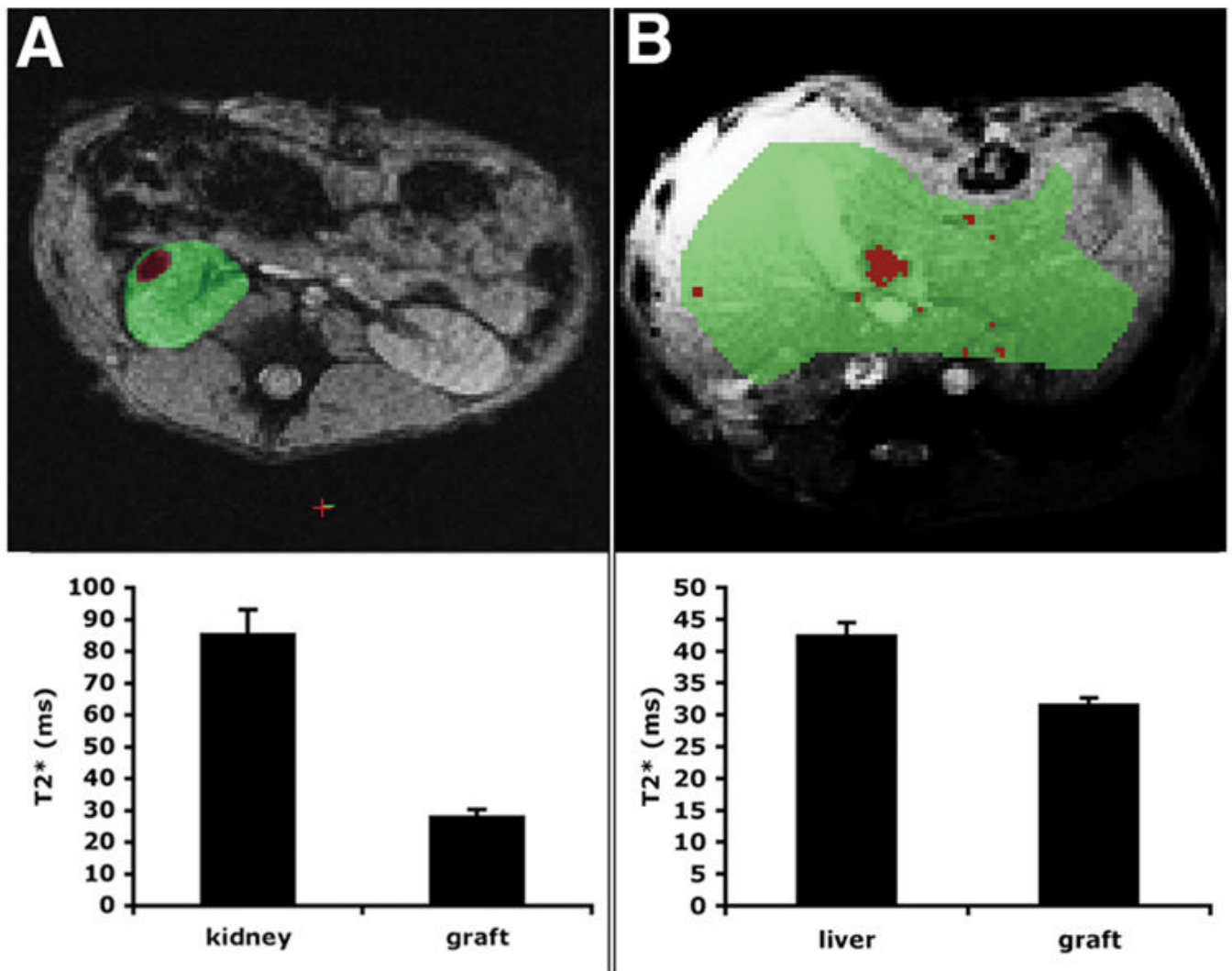


**Figure 3.**

MR image segmentation for assessment of relative transplanted islet mass in the kidney (A) and liver (B) transplantation models. A region of interest (ROI) was drawn manually around the kidney or liver. An automated algorithm was used to segment the ROI into kidney/liver parenchyma (green) and islet graft (red) based on T2\* values. Representative images (top) and the corresponding T2\* values  $\pm$  SD (bottom) are shown. The differential between the two labels was sufficiently large in order to reliably identify the graft ( $p < 0.05$ ). The images are derived from animal B173.

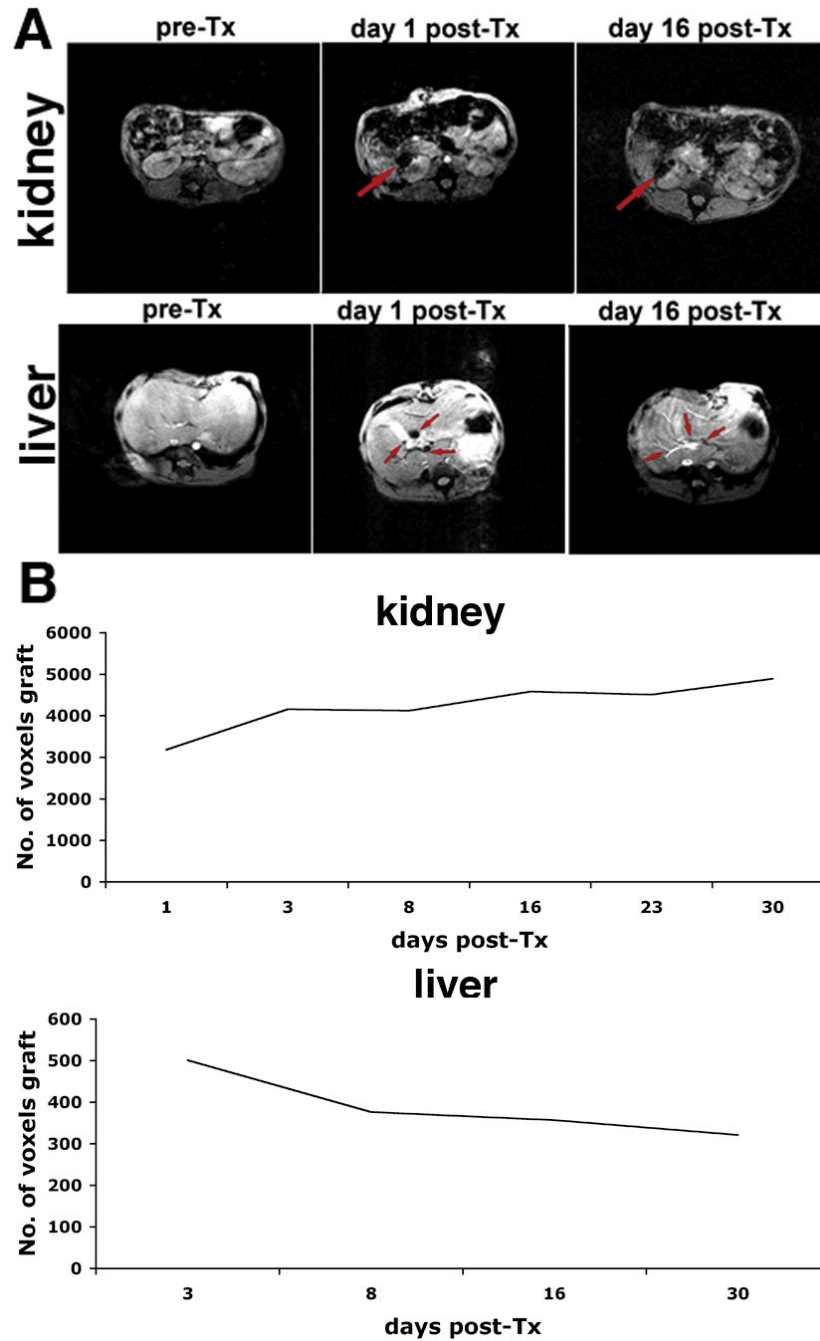


**Figure 4.** Longitudinal MR imaging of labeled autologous islets transplanted into the right renal capsule (top) and the liver (bottom) of a baboon (animal B173). **A:** Pre-transplant images of the liver and kidney do not show signal voids, representative of labeled islets. The right renal islet graft site appears as a large pocket of signal loss. Arrows point to the graft. In the liver, MR imaging reveals distinct foci of signal loss, corresponding to labeled islets along the vascular branches. **B:** Semi-quantitative assessment of graft longevity indicates relative graft stability over 16 days after transplantation.

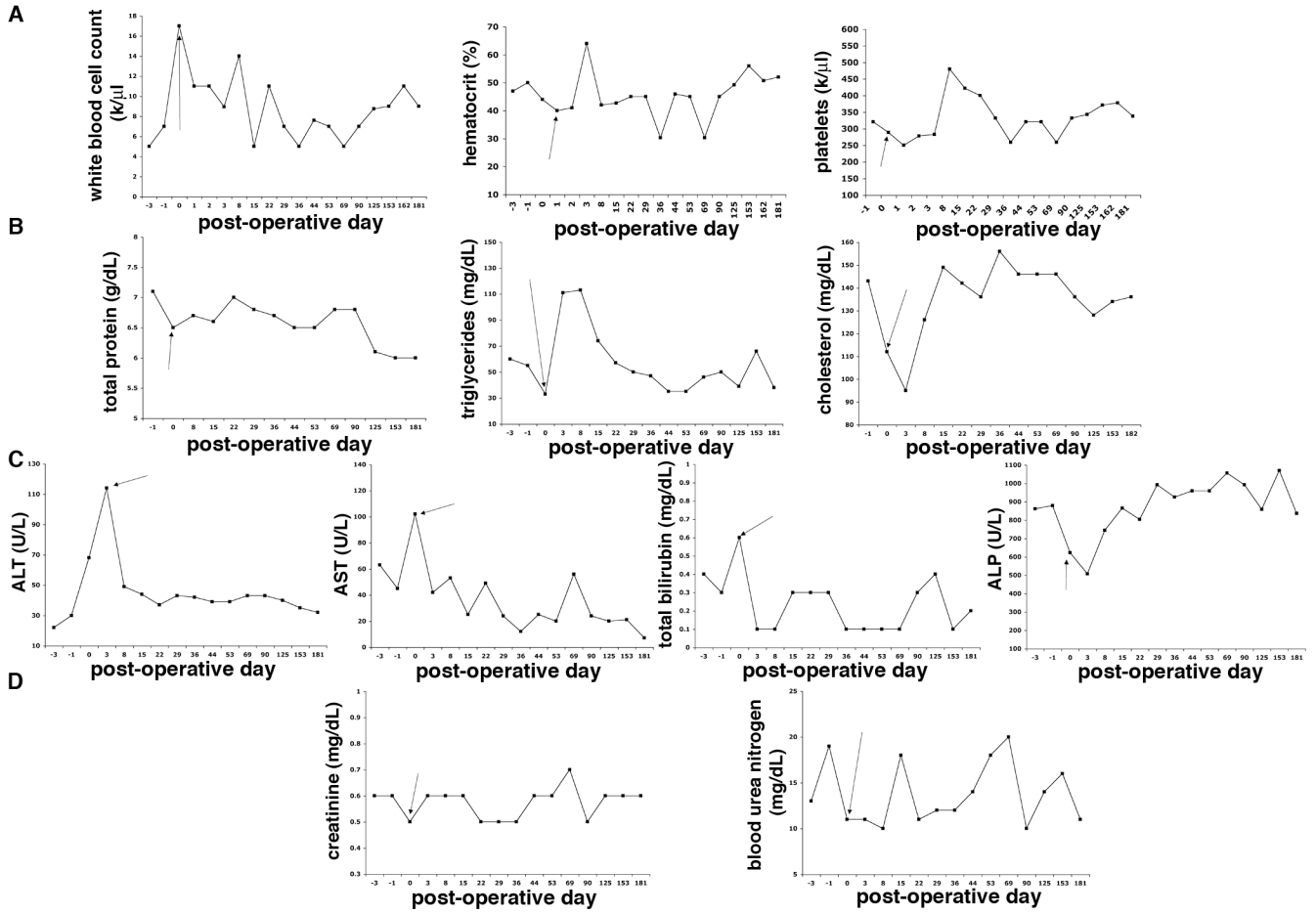


**Figure 5.** Long-term safety profile of transplanted labeled islets (B173). A: Red blood cell count, white blood cell count, platelet count, and hematocrit values remained within normal range, apart from transient changes associated with the transplantation procedure. B: The animals showed normal total protein levels and normal cholesterol and triglyceride levels, besides transient deviation around the time of transplantation. C: Liver function tests (aspartate aminotransferase, AST; alanine aminotransferase, ALT; total bilirubin, and alkaline phosphatase, ALP) were normal, apart from transient deviations from the norm associated with the transplantation procedure. D: Renal function tests (blood urea nitrogen and creatinine) remained normal during follow-up. Results shown are representative of both animals. Arrow points to the day of islet transplantation.

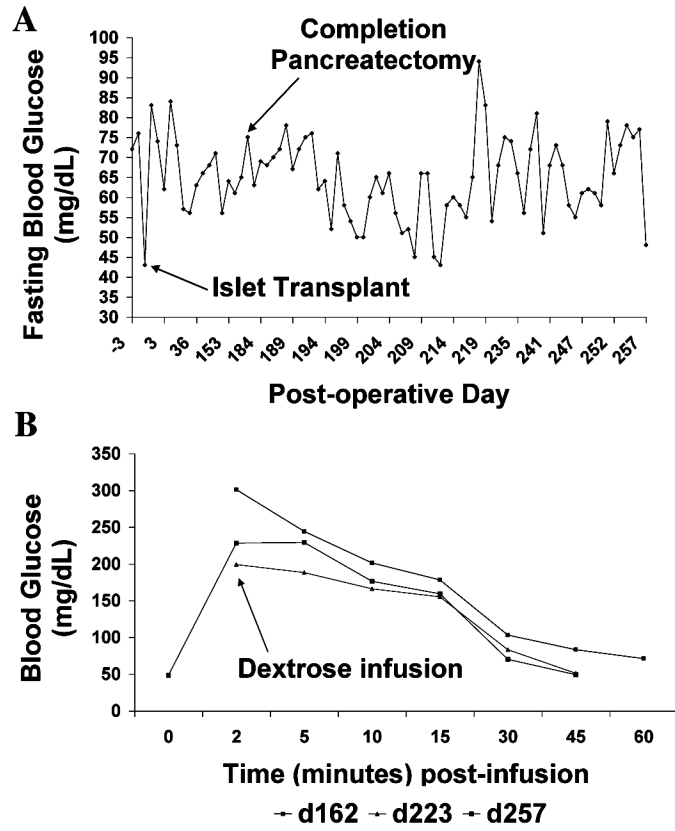


**Figure 6.** Long-term functionality of transplanted labeled islets (B173). Fasting blood glucose (A) and intravenous glucose tolerance (B) remained normal and unchanged before and after completion pancreatectomy, indicating that the labeled grafts were sufficient to maintain glucose homeostasis. Results shown are representative of both animals.